Spatial fingerprint of quantum path interferences in high order harmonic generation

F. Schapper[1,3]*, M. Holler[1,3], T. Auguste[2], A. Zaïr[1], M. Weger[1], P. Salières[2], L. Gallmann[1], and U. Keller[1]

[1]*Physics Department, ETH Zurich, 8093 Zurich, Switzerland*
[2]*CEA-Saclay, IRAMIS, Service des Photons, Atomes et Molécules, 91191 Gif-sur-Yvette, France*
[3]*Both of these authors contributed equally to this work.*
**schapper@phys.ethz.ch*

Abstract: We have spatially and spectrally resolved the high order harmonic emission from an argon gas target. Under proper phase matching conditions we were able to observe for the first time the spatial fine structure originating from the interference of the two shortest quantum paths in the harmonic beam. The structure can be explained by the intensity-dependent harmonic phase of the contributions from the two paths. The spatially and spectrally resolved measurements are consistent with previous spatially integrated results. Our measurement method represents a new tool to clearly distinguish between different interference effects and to potentially observe higher order trajectories in the future with improved detection sensitivity. Here, we demonstrate additional experimental evidence that the observed interference pattern is only due to quantum-path interferences and cannot be explained by a phase modulation effect. Our experimental results are fully supported by simulations using the strong field approximation and including propagation.

OCIS codes: (270.1670) Coherent optical effects; (270.6620) Strong-field processes.

References and links

1. A. McPherson, G. Gibson, H. Jara, U. Johann, T. S. Luk, I. A. McIntyre, K. Boyer, and C. K. Rhodes, "Studies of multiphoton production of vacuum-ultraviolet radiation in the rare gases," J. Opt. Soc. Am. B **4**(4), 595 (1987).
2. M. Ferray, A. L'Huillier, X. F. Li, L. A. Lompre, G. Mainfray, and C. Manus, "Multiple-harmonic conversion of 1064 nm radiation in rare gases," J. Phys. B **21**(3), 001 (1988).
3. X. F. Li, A. L'Huillier, M. Ferray, L. A. Lompré, and G. Mainfray, "Multiple-harmonic generation in rare gases at high laser intensity," Phys. Rev. A **39**(11), 5751–5761 (1989).
4. P. B. Corkum, "Plasma perspective on strong field multiphoton ionization," Phys. Rev. Lett. **71**(13), 1994–1997 (1993).
5. K. C. Kulander, K. J. Schafer, and J. L. Krause, "Dynamics of short-pulse excitation, ionization and harmonic Conversion," NATO Advanced Research Workshop on SILAP (Super-Intense Laser-Atom Physics), (1993).
6. M. Lewenstein, Ph. Balcou, M. Yu. Ivanov, A. L'Huillier, and P. B. Corkum, "Theory of high-harmonic generation by low-frequency laser fields," Phys. Rev. A **49**(3), 2117–2132 (1994).
7. K. Schiessl, K. L. Ishikawa, E. Persson, and J. Burgdorfer, "Wavelength dependence of high-harmonic generation from ultrashort pulses," J. Mod. Opt. **55**(16), 2617–2630 (2008).
8. M. Lewenstein, P. Salières, and A. L'Huillier, "Phase of the atomic polarization in high-order harmonic generation," Phys. Rev. A **52**(6), 4747–4754 (1995).
9. A. Zaïr, M. Holler, A. Guandalini, F. Schapper, J. Biegert, L. Gallmann, U. Keller, A. S. Wyatt, A. Monmayrant, I. A. Walmsley, E. Cormier, T. Auguste, J. P. Caumes, and P. Salières, "Quantum path interferences in high-order harmonic generation," Phys. Rev. Lett. **100**(14), 143902 (2008).
10. M. Holler, A. Zaïr, F. Schapper, T. Auguste, E. Cormier, A. Wyatt, A. Monmayrant, I. A. Walmsley, L. Gallmann, P. Salières, and U. Keller, "Ionization effects on spectral signatures of quantum-path interference in high-harmonic generation," Opt. Express **17**(7), 5716–5722 (2009).
11. P. Salières, B. Carré, L. Le Déroff, F. Grasbon, G. G. Paulus, H. Walther, R. Kopold, W. Becker, D. B. Milosević, A. Sanpera, and M. Lewenstein, "Feynman's path-integral approach for intense-laser-atom interactions," Science **292**(5518), 902–905 (2001).

#121033 - $15.00 USD Received 7 Dec 2009; revised 21 Jan 2010; accepted 24 Jan 2010; published 27 Jan 2010

12. Ph. Balcou, P. Salières, A. L'Huillier, and M. Lewenstein, "Generalized phase-matching conditions for high harmonics: The role of field-gradient forces," Phys. Rev. A **55**(4), 3204–3210 (1997).
13. Ph. Balcou, A. S. Dederichs, M. B. Gaarde, and A. L'Huillier, "Quantum-path analysis and phase matching of high-order harmonic generation and high-order frequency mixing processes in strong laser fields," J. Phys. At. Mol. Opt. Phys. **32**(12), 2973–2989 (1999).
14. M. B. Gaarde, F. Salin, E. Constant, Ph. Balcou, K. J. Schafer, K. C. Kulander, and A. L'Huillier, "Spatiotemporal separation of high harmonic radiation into two quantum path components," Phys. Rev. A **59**(2), 1367–1373 (1999).
15. T. Auguste, P. Salières, A. S. Wyatt, A. Monmayrant, I. A. Walmsley, E. Cormier, A. Zair, M. Holler, A. Guandalini, F. Schapper, J. Biegert, L. Gallmann, and U. Keller, "Theoretical and experimental analysis of quantum path interferences in high-order harmonic generation," Phys. Rev. A **80**(3), 033817 (2009).
16. M. Bellini, C. Lyngå, A. Tozzi, M. B. Gaarde, T. W. Hänsch, A. L'Huillier, and C. G. Wahlström, "Temporal coherence of ultrashort high-order harmonic pulses," Phys. Rev. Lett. **81**(2), 297–300 (1998).
17. C. Corsi, A. Pirri, E. Sali, A. Tortora, and M. Bellini, "Direct interferometric measurement of the atomic dipole phase in high-order harmonic generation," Phys. Rev. Lett. **97**(2), 023901 (2006).

1. Introduction

High order harmonic generation (HHG), a coherent up-conversion process, has been widely studied ever since its first experimental observations [1–3]. The high harmonic generation process is well described by the semi-classical three-step model [4,5]. In a first step, the atomic potential is bent by the strong electric field of the laser pulse, which allows for tunneling ionization of the atom. The freed electron is subsequently quivering in the electric field. Depending on the instant of ionization, the electron can return to its parent ion and possibly recombine to the ground state. This recombination is accompanied by the emission of a high-energy photon. This semi-classical model predicts that, in the plateau region, different electron trajectories lead to the same harmonic photon energy. This was further confirmed and expanded by quantum mechanical calculations [6] that identified the different quantum paths contributing to the emission of a given harmonic order. These paths are a generalization of the classical electron trajectories in the form of complex trajectories. It was predicted that the contributions from these different paths should interfere in the high harmonic emission with the phases accumulated during the corresponding electron trajectories. These quantum path interferences (QPI) could thus be controlled by varying the laser parameters such as its wavelength [7] or intensity [8]. However, no experimental observation was reported until recently due to the spatial and temporal averaging in the usual macroscopic generation conditions that smeared out the interference pattern. In 2008, we reported the first observation of the intensity dependence of the QPI by properly selecting phase matching and spatial filtering conditions [9]. In follow-up experiments performed in different gases, we investigated the influence of ionization effects on the observed interference patterns and could identify the signatures of microscopic and macroscopic processes [10]. Here, we extend our studies to the spatial domain and report the first observation of spatially and spectrally resolved QPI as a function of intensity. Our experimental setup gives both, spectral resolution along one transverse axis of the harmonic beam and spatial resolution along the orthogonal transverse direction. We therefore gain access to both, the spatial fingerprint of the QPI and the intensity-dependent spectral QPI structures studied in our previous experiments. A theoretical model [8,11] based on the strong-field approximation (SFA) and including propagation reproduces the experimental data very well and aids its interpretation.

Theoretical and experimental analysis show that the two shortest electron quantum paths give the main contributions to the harmonic emission, referred to as "short" and "long" trajectories according to their excursion time. This is the result of both, the three-step process occurring on a single-atom level and the macroscopic effect of phase matching [12–14]. Both trajectories contribute macroscopically when the generation medium is placed before the laser focus. The emission resulting from the short trajectory presents a small beam divergence while the contribution of the long trajectory, mainly emitted off-axis, exhibits a larger divergence. Because the relative phase between the interfering high harmonic contributions depends on intensity, we expect a spatial structure for the QPI resulting from the beam profile

#121033 - $15.00 USD Received 7 Dec 2009; revised 21 Jan 2010; accepted 24 Jan 2010; published 27 Jan 2010

of the driving laser. With spatially resolved HHG we have fully resolved this spatial interference structure, and followed its alteration as a function of the laser peak intensity.

2. Theoretical background

In the following, we briefly summarize the QPI theory with respect to their spatial properties. A more detailed discussion of QPI theory can be found in References [9] and [15].

The occurrence of an interference pattern between contributions of different quantum paths can be explained as follows: The phase $\phi_q^{(j)}$ of the quantum path j contributing to harmonic order q is approximately proportional to the ponderomotive potential U_p times the electron excursion time $\tau_q^{(j)}$,

$$\phi_q^{(j)}(r,t) \approx -U_p \tau_q^{(j)} \approx -\alpha_q^{(j)}(I(r,t)) \cdot I(r,t) \approx -\alpha_q^{(j)}(I) I_0 \exp\frac{-2r^2}{w^2} \exp\frac{-2t^2}{\tau^2}, \quad (1)$$

where the laser beam has a peak intensity of I_0, a spatial size of w and a temporal width of τ.

In the plateau region, $\alpha_q^{(j)}$ is a slowly varying function of the laser intensity I [13]. Since $\alpha_q^{(2)} > \alpha_q^{(1)} > 0$, the phase associated to the long path (characterized by a long excursion time, $j = 2$) varies much more rapidly than that of the short path (characterized by a short electron excursion time, $j = 1$). This leads to a complicated interference pattern in space and time during the HHG process. However, it is possible to understand the qualitative signature of QPI in space and time by disentangling the two dimensions as follows.

In the spatial domain, the radial variation of the laser intensity leads to a spatial dependence of the harmonic phase difference $\Delta\phi_q(r) = \phi_q^{(1)} - \phi_q^{(2)} \approx \Delta\alpha_q I(r)$, which results in modulations of the harmonic yield along the spatial coordinate through interference. Another way of looking at this is to consider that Eq. (1) results in a phase front curvature of the harmonic beam that depends on the trajectory:

$$\phi_q^{(j)}(r) \approx -\alpha_q^{(j)} I_0 + \frac{2\alpha_q^{(j)} I_0}{w^2} r^2 \quad (2)$$

for the central part of the beam where $r < w$. The interference of these two different phase fronts in the far field results in an annular fringe pattern. This pattern obviously changes with time as the laser intensity varies in the laser pulse.

In the temporal domain, Eq. (1) results in a phase modulation – a chirp – of the harmonic emission, which is the stronger the longer the trajectory is:

$$\begin{aligned} \Delta\omega(t) &= -\frac{\partial\phi_q^{(j)}(t)}{\partial t} = \frac{\partial\alpha_q^{(j)}(I(t))}{\partial I}\frac{\partial I(t)}{\partial t} \cdot I(t) + \alpha_q^{(j)}(I(t)) \cdot \frac{\partial I(t)}{\partial t} \\ &\approx \alpha_q^{(j)} \cdot \frac{\partial I(t)}{\partial t} \approx -\frac{4\alpha_q^{(j)} I_0}{\tau^2} t. \end{aligned} \quad (3)$$

This harmonic chirp maps the time to a frequency shift in the harmonic spectrum. The emission generated by the leading or trailing edge of the pulse is thereby mapped to higher or lower energy respectively. At the temporal peak of the laser pulse, the exact harmonic frequency is created because $\frac{\partial I(t)}{\partial t} = 0$ [Eq. (3)].

In addition, spatio-temporal effects appear. Since the contributions from the temporal wings are generated with lower spatial peak intensity, they should appear with a smaller divergence in the recorded far-field pattern [see Eq. (2)]. One thus expects that the spatial

#121033 - $15.00 USD Received 7 Dec 2009; revised 21 Jan 2010; accepted 24 Jan 2010; published 27 Jan 2010

extent of the harmonic beam will be largest at the central harmonic frequency and will decrease on both spectral sides.

By spatially and spectrally resolving the harmonic emission, it should be possible to observe the QPI in the two dimensions.

3. Experimental setup

In our experiments (Fig. 1), near infrared laser pulses centered at 800 nm wavelength with a duration of 30 fs and a pulse repetition rate of 1 kHz have been focused into an argon gas jet by a spherical mirror (ROC = 500 mm).

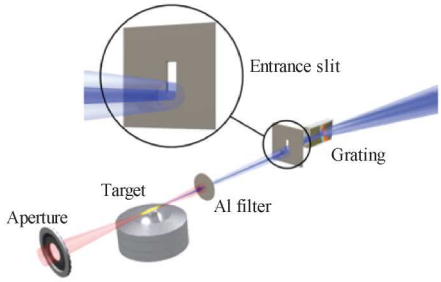

Fig. 1. Experimental setup: The incoming laser beam passes through an aperture and is focused into a pulsed argon jet. The harmonics propagate through an Al foil that filters out the intense generating laser beam. The strong center part of the harmonic emission is cut by the entrance slit of the spectrometer.

The laser peak intensity was changed from $6.0 \cdot 10^{13}$ W/cm^2 to $3.3 \cdot 10^{14}$ W/cm^2 by using a variable attenuator (half-wave plate and polarizer). To find proper phase matching conditions, we adjusted both, the input beam aperture and the position of the gas jet along the propagation direction of the laser. In all our measurements, the gas jet was placed before the laser focus. Once an optimal configuration was found, it was left unchanged for all intensities. The emitted harmonic radiation hit the vertical 1-cm high slit of a XUV spectrometer (McPherson 248/310G) placed 1 m behind the jet. Spatial resolution was obtained with a 2-dimensional CCD detector. We adjusted the weight of the different quantum path contributions by moving the incoming beam in the vertical direction (corresponding to the slit direction) and therefore controlling the portion of the beam entering the spectrometer. Blocking the intense central part of the harmonic beam resulted in an increased visibility of the weaker parts with high divergence.

4. Results

Spatially and spectrally resolved harmonics have been measured for different laser intensities. To clarify the general behavior, we first discuss a spectrum recorded at fixed laser intensity. The spatially resolved spectrum shown in Fig. 2(a) was recorded at a fixed peak intensity of $3.3 \cdot 10^{14}$ W/cm^2 in argon. Each spectral component plotted along the horizontal axis is spatially resolved along the vertical axis. We have observed spatial and spectral modulations of the harmonic yield. The areas with constructive interference create a parabolic structure: Moving from the blue side of the harmonics to the exact harmonic frequency to the red side, these areas first increase in divergence, reach their maximum and decrease again. Applying the time-to-frequency mapping of the harmonic chirp, one sees that these areas increase in divergence on the leading edge of the pulse until the temporal peak of the pulse is reached, and then decrease in divergence on the trailing edge. Since the harmonic phase difference $\Delta\phi_q(t) \approx \Delta\alpha_q \cdot I(t)$ is proportional to $I(t)$, the parabolic shape is to be expected close to the maximum of the laser envelope where the harmonics are emitted.

#121033 - $15.00 USD Received 7 Dec 2009; revised 21 Jan 2010; accepted 24 Jan 2010; published 27 Jan 2010

The interference structure disappears for a jet positioned after the laser focus where the short quantum path dominates the emission. The latter holds true also for the center part of the beam, which is orders of magnitude more intense even for a jet positioned before the laser focus. It was therefore crucial to suppress this part of the beam. However, the very low signal makes it very difficult to measure the spatial fringe pattern. Our experimental results are reproduced by SFA calculations and consecutive propagation of the electric fields. In Fig. 2(b) a calculated spatially resolved harmonic spectrum is shown for a fixed laser peak intensity of $2.5 \cdot 10^{14}$ W/cm^2. A fringe pattern very similar to the measured one is obtained. To our knowledge, this is the first time that QPI is observed *inside* the harmonic beam, and not as a variation of the beam properties. Indeed, when the laser intensity is varied, the fringe pattern is altered: the rings move outwards as the intensity increases [see Media 1 and Fig. 3(a)]. In an earlier experiment, the harmonic beam was integrated within an off-axis spatial filter window, and we measured the modulations of the harmonic yield with laser intensity as the rings of the QPI interference pattern were moving across the spatial filter [9]. We were thus measuring the *variation* of the pattern, not the pattern itself. This is a significant step towards a full characterization of the harmonic emission. Note that QPI leads to an annular interference pattern that is very different from the fringe pattern resulting from two spatially separated sources. The latter exhibits vertical stripes in the beam profile and was used in, e.g., [16,17] to get information on the phase of the quantum paths through the interference of contributions from the same quantum path (short or long) from the two separate sources. However, no interference of contributions from the short trajectory with contributions from the long trajectory was reported.

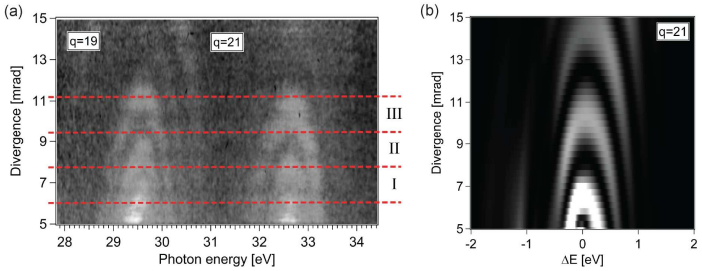

Fig. 2. (a) Measured [see Media 1 for different laser intensities] and (b) simulated result. Spatially resolved harmonic spectrum (a) measured for harmonic orders 19 and 21 at a fixed intensity of $3.3 \cdot 10^{14}$ W/cm^2 and (b) simulated for harmonic 21 at a peak intensity of $2.5 \cdot 10^{14}$ W/cm^2.

By recording spatially resolved spectra for different laser peak intensities and then performing a numerical integration over an interval in the spatial direction, we can reproduce these previous results as shown in Fig. 3(b). Please note that in the current experiment our spatially resolving spectrometer has less dynamic range since is uses a MCP with phosphor screen which is then imaged to a CCD sensitive in the visible instead of direct detection by an XUV CCD. The spatial window used for the integration is indicated by the red lines in Fig. 2(a). A corresponding line-cut at the exact harmonic frequency then shows modulations of the harmonic yield with laser intensity.

In Fig. 4, three non-overlapping integration windows for harmonic 21 (areas marked in Fig. 2(a) by I, II, III) were chosen. Moving the integration area to higher divergence (from region I to III) shifts the modulations to higher intensities and the modulation period increases. A possible interpretation is that the harmonic emission in the outer part of the beam (high divergence) was created with a lower effective intensity. This is the case if the curvature of the harmonic phase front is that large at the exit of the generating medium that the spatial pattern is directly projected into the far field. As a consequence, the contributions in the observed far-field spatial regions are generated at a position in the spatial wings of the laser

#121033 - $15.00 USD Received 7 Dec 2009; revised 21 Jan 2010; accepted 24 Jan 2010; published 27 Jan 2010

pulse $r^{(1)} = r^{(2)} \neq 0$ where the intensity is lower than the peak intensity. One then expects that the resulting QPI modulations will be shifted to higher peak intensity (and their period will be increased) as compared to the modulations in the inner part of the harmonic beam generated at r closer to 0. If the phase front curvatures of contributions from the short and the long quantum path are sufficiently different, one may even consider that they originate from two different positions $r^{(1)} \neq r^{(2)}$ within the medium such that $\Delta\alpha = \Delta\alpha_q(I(r^{(1)},t), I(r^{(2)},t))$.

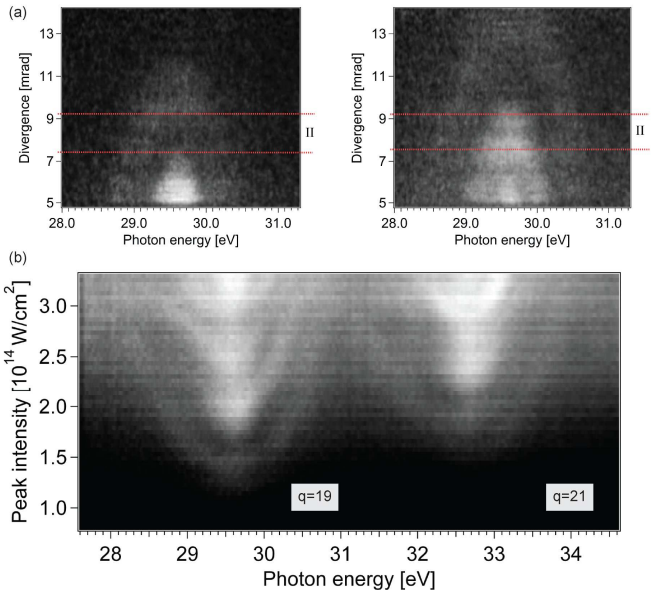

Fig. 3. (a) Spatially resolved spectrum of harmonic 21 spectrum for a laser peak intensity of $1.6 \cdot 10^{14}$ W/cm^2 (left) and $2.0 \cdot 10^{14}$ W/cm^2 (right); (b) Harmonic signal integrated from 7.5 to 9.2 mrad [area II in (a) and in Fig. 2(a)] along the spatial coordinate.

When the harmonic dipole is restricted to the short ($\tau_q^{(1)} \approx T/2$, $\alpha_q^{(1)} \approx 1 - 5 \cdot 10^{-14}$ rad cm^2/W) and the long ($\tau_q^{(2)} \approx T$, $\alpha_q^{(2)} \approx 20 - 25 \cdot 10^{-14}$ rad cm^2/W) trajectory (T being the oscillation period of the laser field), the theoretically expected interference period of the two first quantum paths is $2\pi/\Delta\alpha \approx 3 - 4 \cdot 10^{13}$ W/cm^2. This is in excellent agreement with our experimental observations for a spatial integration window close to the center of the beam. The measured periodicity for a spatial integration window marked with I in Fig. 2(a) is $4 \cdot 10^{13}$ W/cm^2. This periodicity increases to $7 \cdot 10^{13}$ W/cm^2 for the integration window marked with III. For higher harmonic orders in the cutoff region, modulations are not observed because only one trajectory contributes to the emission (data not shown). We can thus conclude that the behavior observed in the numerically integrated spatially resolved data is consistent with our results previously published in Ref [9]. and [10].

In addition to our confirmed previous observations, spatial resolution of the QPI spectra should give us access to faster oscillation periods resulting from higher order electron trajectories that could be averaged out by the spatial integration. Fourier analysis of our data however did not clearly reveal such signatures. A possible reason for the absence of higher order modulations in the Fourier transform of the QPI data could be the relatively low signal-to-noise ratio of our data that prevents us from detecting the theoretically predicted weak contribution of higher order trajectories. Indeed, the quantum diffusion during their long excursion time results in a much lower recombination probability compared to the two shortest trajectories.

#121033 - $15.00 USD Received 7 Dec 2009; revised 21 Jan 2010; accepted 24 Jan 2010; published 27 Jan 2010

Another benefit of spatially resolved measurements is that they provide a means to identify a possible contribution to intensity-dependent modulations of the harmonic yield which is not due to QPI. Slow spectral modulations appear [15] when the single-atom response is calculated with SFA using only the shortest trajectory. These modulations cannot be attributed to QPI, but are a direct consequence of the harmonic phase modulation. All frequencies apart from the exact harmonic frequency can be generated at two different instants of time within the laser pulse envelope leading to a possible interference between these contributions. However, this is simply a spectral redistribution of the frequency components and does not affect the spectrally integrated signal. Therefore, the spatially resolved emission gives us an accurate tool to distinguish between QPI and interference due to phase modulations: the latter should disappear when spectrally integrating the spatially-resolved signal, while QPI modulations should persist (with a decreased contrast due to the temporal averaging over the envelope of the laser pulse).

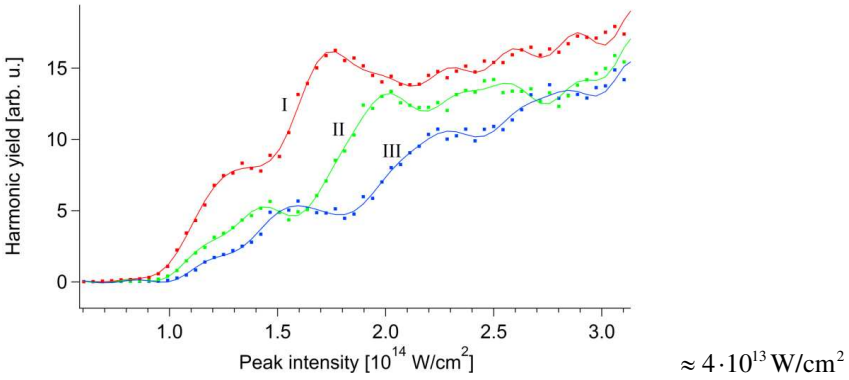

Fig. 4. Harmonic yield versus laser intensity for three different spatial integration windows [marked in Fig. 2(a)] for harmonic order 21 (measured data shown as dots, lines show smoothed data).

In Fig. 5(a) a spatially integrated spectrum with an integration window of 5.80 to 5.88 mrad is shown. This small spatial integration was performed just to increase the signal to noise ratio. When spectrally integrating harmonic 19, the harmonic signal is still modulated with a periodicity of , as can be seen in Fig. 5(b). As a result, phase modulation can be excluded as the origin for the appearance of an interference structure.

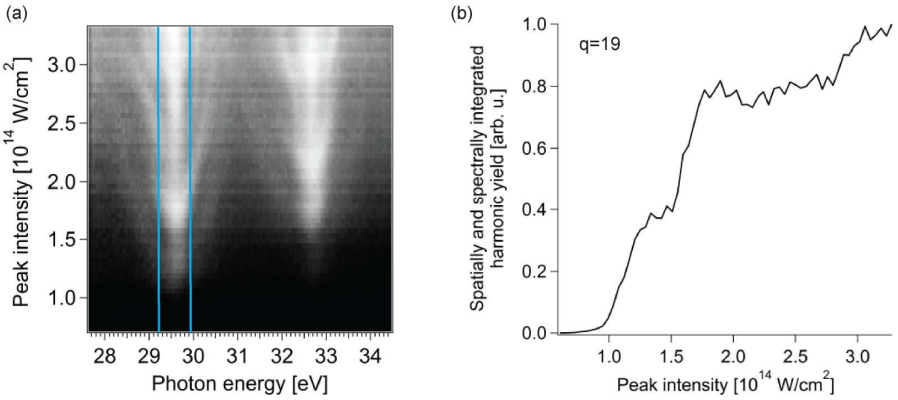

Fig. 5. (a) spatially integrated (5.80 – 5.88 mrad) yield for harmonic 19 and 21 and (b) spectral integration over area indicated in (a). The spectrally integrated yield is still modulated with a periodicity of $\approx 4 \cdot 10^{13}\,\mathrm{W/cm^2}$ which is a clear indication for QPI.

#121033 - $15.00 USD Received 7 Dec 2009; revised 21 Jan 2010; accepted 24 Jan 2010; published 27 Jan 2010

5. Conclusion

By recording spatially resolved spectra of high order harmonics generated in argon, we found fingerprints of quantum path interference between the two shortest quantum paths. Our measurements represent the first observation of QPI *inside* the harmonic beam. The parabolic structure of the spatially and spectrally resolved emission can be explained by the intensity dependence of the harmonic phase of the two trajectories and the corresponding time-to-frequency mapping. Our experimental results underline the necessity of spatial filtering and blocking of the central part of the beam to observe the QPI and are fully supported by simulations including SFA-calculation of the single-atom response and propagation of the electric fields in the macroscopic medium.

When performing a – partial – spatial integration of the signal, we find that the modulation period of the QPI increases when moving the integration window to higher divergence. We attribute this behavior in the outer region of the harmonic beam to the generation of the signal at a position in the spatial wings of the laser beam (or even at two different positions) with lower effective intensity than the peak intensity. Furthermore, we can reproduce our previously reported measurements [9,10] when integrating the spatially resolved signal over the same window.

By spectrally integrating the harmonic yield, we rule out the phase modulation as the origin for the occurrence of interference fringes that are thus unambiguously attributed to QPI.

With improved signal-to-noise levels, our method has the potential to be a sensitive detector for QPI contributions from higher order electron trajectories and may thus yield first direct experimental evidence for such higher order contributions to high order harmonic generation.

Acknowledgement

This research was supported by the NCCR Quantum Photonics (NCCR QP), research instrument of the Swiss National Science Foundation (SNSF), the French Agence Nationale de la Recherche (ANR-09-BLAN-0031-01, ATTO-WAVE), COST-STSM-P14-01910, and the European Commission through the RTN XTRA (MRTN-CT-2003-505138).

#121033 - $15.00 USD Received 7 Dec 2009; revised 21 Jan 2010; accepted 24 Jan 2010; published 27 Jan 2010